Annals of the BMVA Vol. 2013, No. 4, pp 1–11 (2013)

Spin-context Segmentation of Breast Tissue Microarray Images

Shazia Akbar[1], Stephen J. McKenna[1], Telmo Amaral[2], Lee Jordan[3], Alastair Thompson[4]

[1]School of Computing,
University of Dundee, UK

[2]Institute of Biomedical Engineering,
University of Porto, Portugal

[3]Pathology,
Ninewells Hospital, Dundee, UK

[4]Dundee Cancer Centre,
Ninewells Hospital, Dundee, UK

*Corresponding author's email address:
⟨shaziaakbar@computing.dundee.ac.uk⟩

Abstract

Tissue microarrays have become an important tool in clinical research to analyse molecular and protein markers in various types of cancer. However their analysis is a time-consuming task and introduces inter- and intra-observer variations. An automated method is proposed, called *spin-context*, to segment *in-situ* and invasive tumour regions in images of breast tissue microarrays. Spin-context incorporates contextual information extracted from images in a rotationally invariant manner. Additionally, the effect of removing background context locations at boundaries of tissue microarray spots is evaluated. Quantitative evaluation is reported using tissue microarray spots stained for estrogen receptor. Results show that incorporating context in this way improves classification performance, particularly around spot boundaries, compared to classification incorporating no context.

1 Introduction

In clinical research, tissue microarrays (TMAs) have become an important tool for high-throughput molecular analysis to analyse various types of cancers [Voduc and Nielsen, 2008, Jawhar, 2009]. The application of TMAs has grown considerably since its origination in 1998 [Kononen et al., 1998]. The most popular use of TMAs is in translational research for

validation of diagnostic markers in annotated clinical samples. As tumour banks are maturing with regard to follow-up data, it is possible to perform correlations of biomarker expression with clinical endpoints such as disease-free survival or overall-survival. In clinical research, TMAs are being used for testing new antibodies and probes, or determining optimal staining conditions.

TMAs are constructed by extracting core samples, typically $0.6mm$ in diameter, from formalin fixed, paraffin embedded tissue blocks and transferring them to a single multicore paraffin block. It is possible for each TMA core to be derived from a different patient or tumour, however, typically multiple cores are taken across a single tumour to provide representation of tumour variability. Typically, a single TMA block represents 40+ patients or tumours. Each TMA block is then sectioned using a microtome to yield approximately 5 micron thick sections, these are floated across a waterbath and each section is lifted onto a separate glass slide. Therefore each slide-mounted TMA section will consist of a monolayer of TMA spots, representing a cross section of the TMA cores mounted within a TMA paraffin embedded block. TMA multi-core block sections are used as an alternative to whole mount slides as they preserve the original tissue block in a condition that is compatible with verification of clinical diagnosis or performing new immunostaining for future diagnostic evaluation [Moch et al., 2001]. TMAs also allow the preservation of patients' archival tissue for future studies which is essential for clinical research.

Currently, analysis of TMAs is not automated and suffers from inter- and intra-observer variations. Furthermore the growth of tissue banks has lead to an increased workload for pathology experts, exceeding the manual skills available. Annotation software for breast tissue histopathology images often requires a pathologist to partially annotate some tissue components in order for the software to then analyse a whole mount slide. This is time consuming. When applied to TMA spots, regions are often mislabelled due to lack of context.

In this paper a method that classifies pixels as tumour (invasive or *in-situ* carcinoma) or non-tumour probabilistically is described. A distribution-based auto-context descriptor called *spin-context* is proposed and results are reported on estrogen-receptor stained TMA spots by comparison to manual segmentation performed by a pathologist. This paper extends previously published work [Akbar et al., 2012].

2 Related Work

Related work on tumour segmentation includes that of [Wang et al., 2011] who propose a method for segmenting tumour, stroma and inflammatory cells in TMA images using tissue architecture extraction and a tumour texture learning model. Tissue architecture extraction consisted of a stain separation method and an unsupervised multistage entropy-based segmentation method. Tumour texture learning consisted of a Markov random field image segmentation system. [Karaçali and Tözeren, 2007] propose a textural analysis algorithm for a multi-classification problem to identify cancer in breast TMA blocks. Textural properties are constructed from three parameters: area of the image occupied by chromatic-rich cell nuclei, area of the image occupied by collagen-rich stroma and spatial heterogeneity.

The auto-context method, described in [Tu and Bai, 2010], is an iterative pixel labelling technique, in which some of the label probabilities output at a given iteration are used as contextual data that are concatenated with local image features to form the input vector for the following iteration. Auto-context has been used for medical image segmentation. [Morra

et al., 2008] used AdaBoost with auto-context to segment hippocampus in 3D structural MRI. [Tu and Bai, 2010] used auto-context to segment multiple structures in brain MRI. [Tao et al., 2009] used Gaussian mixtures with simplified auto-context to segment ground glass nodules in 3D lung CT data. [Montillo et al., 2011] segmented structures such as aorta, pelvis, and lungs in 3D CT data, proposing an extension of decision forest classifiers that incorporates semantic context in a manner similar to auto-context. [Jurrus et al., 2010] described an auto-context method to detect membranes in electron micrographs. None of the above used distribution-based context descriptors and, appropriately for those applications, descriptors were not invariant under image rotation.

In recent work, context has been applied to 2D histopathology images to improve classification of class labels in tissue. [Chomphuwiset et al., 2011] use Hough transform-based techniques to detect cell nuclei in liver histopathology images. They also integrate random forest classification results, obtained from texture features, with context information from nearby nuclei and regions. [Xu et al., 2012] propose a tumour segmentation, clustering and classification method using Multiple Instance Learning (MIL) for colon histopathology images. Contextual information is introduced as a prior for MIL to encourage neighbouring image patches to share similar class labels. However, to the best of the authors' knowledge, context has not been applied to breast histopathology images which contain large variations between samples compared to colon and liver tissue. This introduces difficulties when classifying small areas of tissue such as TMAs. In this paper the problem of tumour segmentation in images of breast TMAs is addressed.

3 Method

The problem of locating (invasive or *in-situ*) carcinoma in images of TMA spots is formulated as classifying each location on a grid as being tumour or non-tumour. The image patch around each location is characterised using local features extracted at full resolution, specifically differential invariants up to 2nd order, [Schmid and Mohr, 1995], and spin intensity image features as described by [Lazebnik et al., 2005]. A method called *spin-context* [Akbar et al., 2012] is proposed which incorporates context in a rotationally invariant fashion, as the rotation of the tissue in histopathology images is arbitrary. Before describing spin-context, auto-context classification and spin intensity image features are briefly described.

3.1 Spin intensity image features

Spin intensity image features were proposed for texture representation, [Lazebnik et al., 2005]. A spin feature encodes the distribution of brightness values within a circular support region centred at a location, $\mathbf{x}_0$, using a histogram representation that is invariant under image rotation. The contribution of a pixel $\mathbf{x}$ depends on its intensity value, $I(\mathbf{x})$, and its distance from $\mathbf{x}_0$, $||\mathbf{x}-\mathbf{x}_0||$, as shown in Equation (1). α and β are parameters that determine bin size in the two-dimensional 'soft' histogram, H, where each bin is indexed by the radial distance interval, d, and intensity interval, i.

$$H_{(d,i)} = \sum_x \exp\left(-\frac{(||\mathbf{x}-\mathbf{x}_0|| - d)^2}{2\alpha^2} - \frac{|I(\mathbf{x}) - i|^2}{2\beta^2}\right) \quad (1)$$

Algorithm 1 Auto-context training.

Given a set of J training images together with their label maps, $S = \{(Y_j, X_j), j = 1...J\}$: For each image X_j , construct a probability map $P_j^{(0)}$ containing K grid locations, with uniform distribution on all the labels. For iteration $t = 1...T$:

1. Make a training set $S_t = \left\{(Y_{jk}, (X_j(N_k), g(P_j^{(t-1)}, k))), j = 1..J, k = 1..K\right\}$ where $X_j(N_k)$ is the image patch and $g(P_j^{(t-1)}, k)$ is the context descriptor centred at the kth location in the jth image.
2. Train a classifier on S_t.
3. Use the trained classifier to compute new classification maps $P_j^{(t)}$ for each training image X_j.

3.2 Auto-context

As stated earlier, auto-context, described in [Tu and Bai, 2010], is an iterative pixel labelling technique, in which label probabilities output at a given iteration are used as contextual data for the following iteration. Contextual data are concatenated with local image features to form input vectors for each iteration. Context locations are identified by applying a star-shaped 'stencil' to label probability maps.

This technique is described in Algorithm 1, where X_j is a 2D image and Y_j is its corresponding ground truth label image. X_j refers to the jth image in the training set and $X_j(N_k)$ denotes the image patch centred at the kth location. g is a function which computes a context descriptor from posterior probability values by selecting locations centred around point k. Posterior probability values are selected from classification map $P_j^{(t-1)}$. Figure 1(a) shows how context locations are selected using a star-shaped stencil, somewhat similar to the stencil adopted in [Tu and Bai, 2010]. The red grid point denotes location k and blue locations are those at which posterior probailities contribute to the context descriptor. In the initial iteration, $P_j^{(0)}$ is a uniform distribution. Both local image features and probability values are input into the classifier for training, which is subsequently used to output an updated classification map for iteration t. The algorithm iteratively updates until convergence, producing a series of T classifiers.

3.3 Spin-context

Tu and Bai used a star shaped 'stencil' to select context location points around the pixel being classified. The resulting context features from this stencil were not invariant under image rotation. By using an alternative, *spin-context*, rotationally invariant context features can be computed for a given grid location from label probability values within a circular support region. Spin-context is extracted analogously to intensity spin features, computing a two-dimensional soft histogram reflecting the distribution of probabilities within the support region, with rows representing probability intervals and columns representing radial distance intervals. Figure 1(b) shows the circular mask used to compute spin-context. Each annulus corresponds to a radial distance interval in the resulting spin-context descriptor. Figure 2 illustrates spin-context for a given support region. In iteration 1, context is not

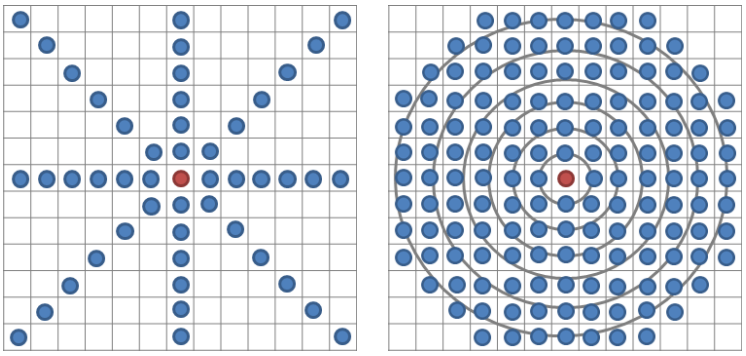

(a) (b)

Figure 1: (a) Star-shaped stencil and (b) circular stencil for selecting context locations from label probability maps.

available from the previous iteration so a uniform constant descriptor is adopted. Therefore, the resulting probability map for the initial iteration does not incorporate context.

3.4 Boundary sensitive spin-context

The spin-context descriptor allows context outside the tissue spot's boundary to be disregarded while considering only context within the spot region. Figure 3 illustrates the advantage of using spin-context to produce a more accurate representation of context information around the boundaries of the spot. The use of boundary information prior to context extraction allows the contributions of out-of-boundary points towards the normalised two-dimensional spin histogram to be ignored. In doing so, not only is context information accurate for the current iteration but subsequent iterations also reflect on accurate information extracted from the spot region. The star-shaped stencil-context descriptor, not being distribution-based, does not allow this level of flexibility to be maintained, resulting in background interference, or the need to handle missing context data.

TMA spot segmentation was performed using Otsu's method, [Otsu, 1979], to threshold greyscale images of TMA spots. Foreground regions were dilated and flood-filled using 8-connected neighbourhoods. Small connected components with areas below a fixed threshold were discarded. The resulting TMA binary segmentation image was used to identify grid locations corresponding to regions containing tissue. Additionally, image patches which overlapped edge boundaries of the TMA spot were modified to only include grid locations containing tissue, as shown in Figure 3.

4 Experiments

TMA spots were subjected to nuclear staining for estrogen receptor (ER). Spot images were 4000×4000 pixels. Data consisted of 64 images, 32 of which contained tumour regions annotated by a highly experienced pathologist and 32 of which were confirmed to contain only benign tissue. Example pathologist annotations are shown in Figure 5.

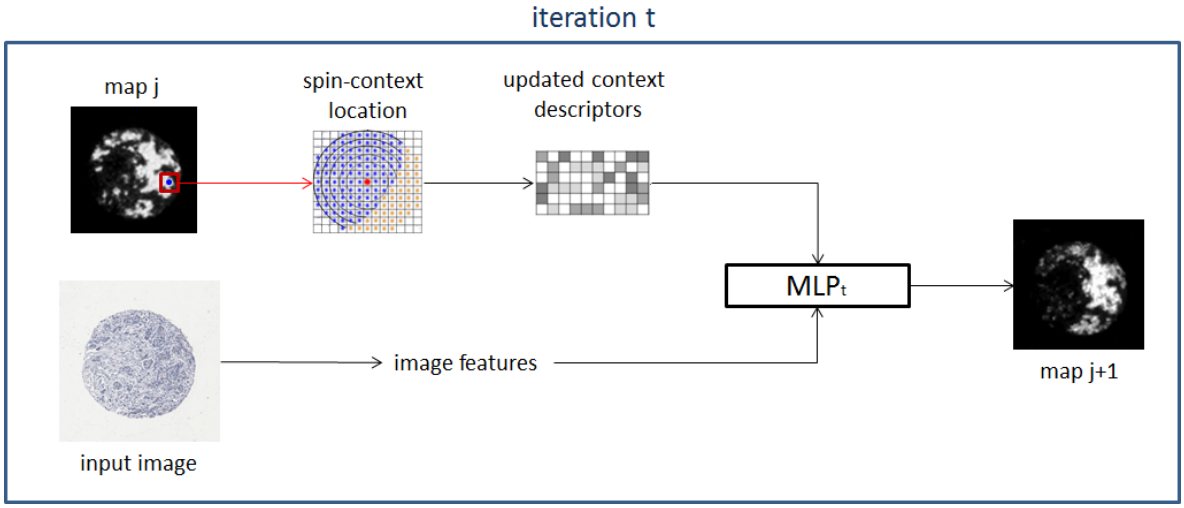

Figure 2: Spin-context constructs context descriptions for a point to be classified (the blue dot) by applying a circular support region centred on that location. The resulting classification map produced by the MLP classifier updates context descriptors iteratively.

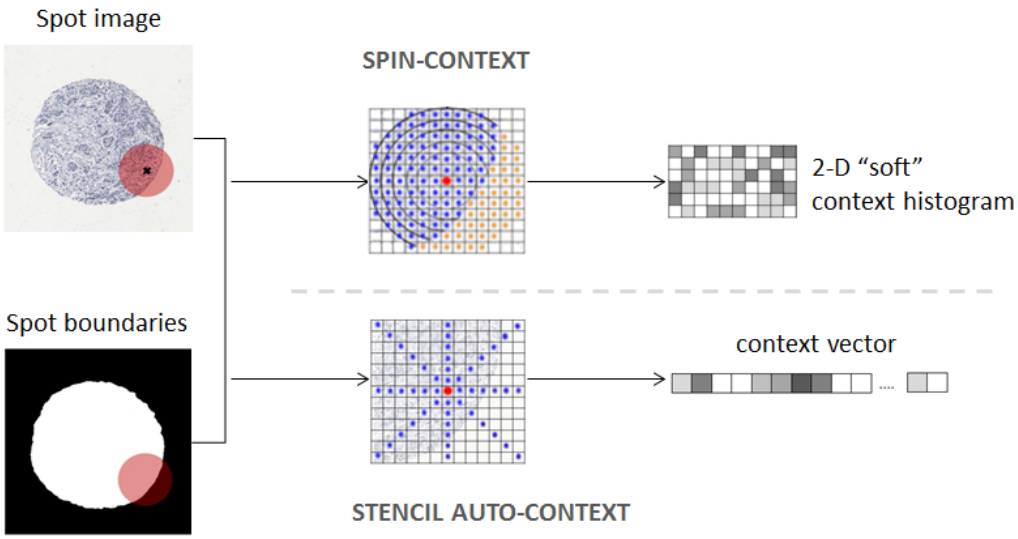

Figure 3: A binary mask is used to ignore the contributions of pixels outside the spot's boundary to the spin histogram. Stencil-context, however, corresponds to label probability values at all locations lying on a star-shaped stencil, regardless of spot boundaries.

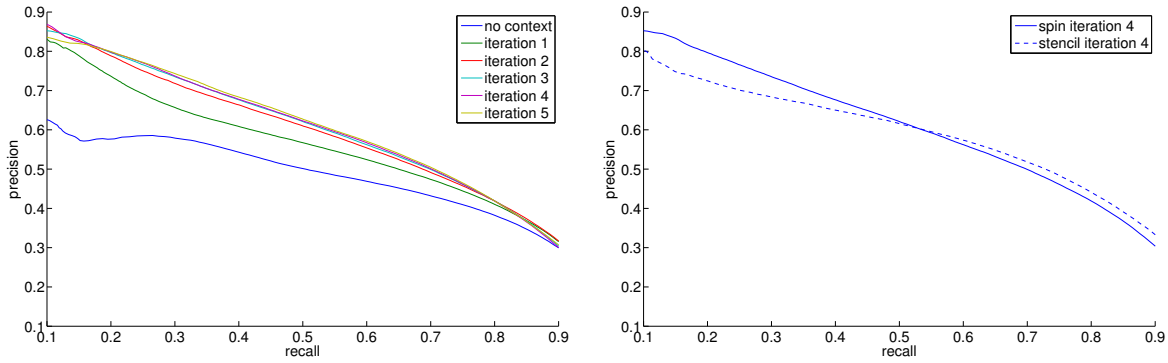

(a) (b)

Figure 4: Precision-recall curves for tumour localisation using spin-context. (a) Effect of five spin-context iterations on MLP classification. (b) Comparison of stencil-context and spin-context for iteration 4 on MLP classification.

Tumour labelling was evaluated using ten-fold cross-validation on the 64 spots. Multi-layer percepton (MLP) classifiers were used with five hidden units, a regularisation constant of 0.1 and scaled conjugate gradient optimisation. MLPs were trained to output class posterior probabilities. Local and context features were computed at points on a 76×76 grid (a grid step of 50 pixels). Differential invariant features were computed at three scales using a Gaussian pyramid and filters with a standard deviation of 8 pixels. Intensity spin local features were computed at two scales (again using a Gaussian pyramid) with a circular support region with a radius of 50 pixels. Spin-context used a circular support region with a radius of six grid points, as shown in Figure 1(b). Auto-context (non-rotationally invariant context) was also evaluated using a stencil in which neighbouring grid points within a radius of six grid spacings in each of the eight cardinal and inter-cardinal compass directions were used as context, as shown in Figure 1(a). Labellings obtained were compared to ground-truth segmentations provided by the pathologist.

5 Results

The precision-recall curve in Figure 4(a) displays the results obtained for six spin-context iterations. Spin-context improved the precision-recall curve, at least in the first two iterations. Compared to a standard MLP classifier which incorporated no context, spin-context improved the precision-recall curve.

Figure 4(b) compares spin-context with stencil-based auto-context. At lower recall values spin-context was superior. At higher recall values the methods were similar. In both cases MLP classifiers were used.

Figure 5 shows three spots, two containing tumour and one not containing tumour, along with their expert annotations and the outputs of the spin-context method. In Figure 5(a), posterior probabilities within tumour regions increased at each iteration, so that after the final iteration they were above 0.9 for most tumour pixels. In Figure 5(b), non-zero probabilities occur within regions of normal tissue at the first iteration; however, their values decreased after further iterations, so that a binarisation of the labelling would result in an almost en-

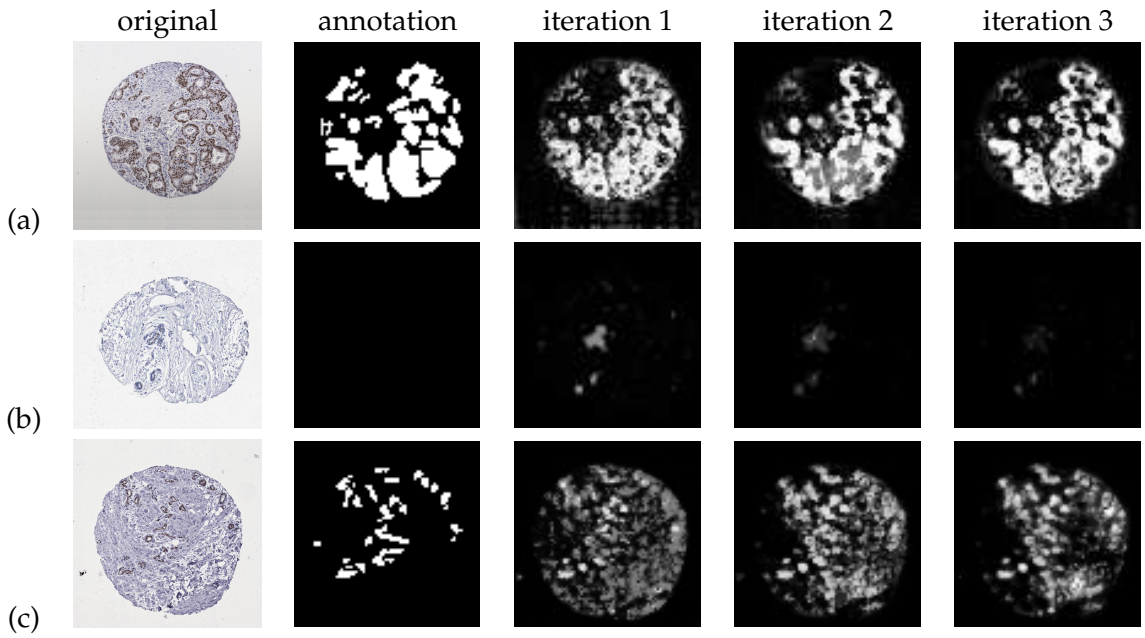

Figure 5: Tumour location probabilities obtained by spin-context. Shown for each TMA spot are the pathologist's annotation, the labelling obtained using local image features (iteration 1) and labellings obtained after incorporating label context (iteration 2 and iteration 3). (a) Invasive cancer labelled largely in agreement with the pathologist. (b) Benign tissue. (c) One of the worst results obtained.

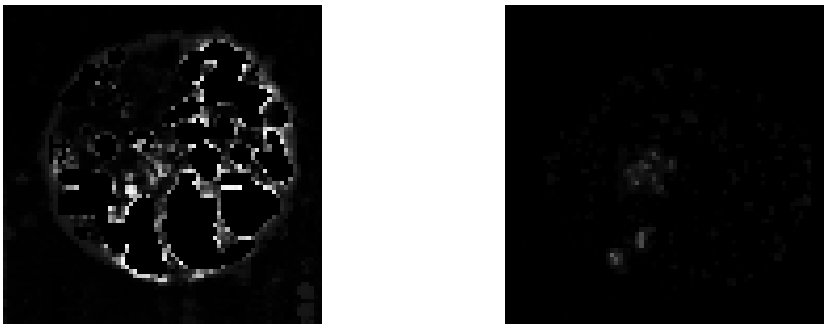

Figure 6: Absolute difference between spin-context after three iterations and pathologist ground truth (i.e. $|\text{spin-context} - \text{ground truth}|$). Results are shown for TMA spots containing (a) tumour and (b) no tumour

tirely empty (i.e. correct) output. Figure 5(c) shows a case of unsuccessful labelling.

Figure 6 shows difference images comparing spin-context results after three iterations with pathologist ground truth. When no tumour is present in Figure 6(b), the comparison with the pathologist annotation is almost identical. However in Figure 6(a) an additional edge around tumour regions is observed in spin-context, resulting in an outline in the difference image. This suggests the majority of errors observed in spin-context are around tumour boundaries.

A second experiment evaluating boundary regions of TMA spots after applying boundary sensitive spin-context is described in Section 3.4. In this experiment background interference is reduced by limiting context locations to spot regions. Results are shown for those grid locations within 150 pixels of the spot boundary. Table 1 shows area under ROC curve (AUC) values obtained within TMA spot boundary regions using MLP with no context, spin-context and an adaptation of spin-context which incorporates context within TMA spot boundaries. In the adaptation of spin-context, context descriptors which reflect contextual properties in regions containing breast tissue (i.e. inner TMA spot regions) are constructed. When no context is incorporated in boundary-sensitive spin-context, background regions are not classified.

	No context	Iteration 1	Iteration 2
Spin-context	0.819	0.841	0.849
Boundary sensitive spin-context	0.831	**0.852**	0.854

Table 1: AUC values obtained within edge boundaries of TMA spots using MLP with no context and spin-context. Results are shown for context extracted from entire images and context limited to spot regions, thereby ignoring background regions.

The use of context around spot boundaries after one iteration of boundary-sensitive spin-context is comparable to the result achieved after two iterations of the original implementation of spin-context. This suggests the use of TMA spot boundaries can reduce computational costs associated with spin-context. In all cases, spin-context improves performance compared to a standard MLP classification approach which incorporates no context.

Table 1 shows that a simple segmentation of TMA spots can increase performance around the boundaries of TMA spots by eliminating background interference in context descriptors.

6 Conclusion

A tumour segmentation method, spin-context, was presented incorporating rotationally invariant context features. It was validated against manual annotations provided by a trained pathologist. Figure 5 shows how spin-context can be useful to pathology research in locating tumour regions. Evaluation shows that spin-context improves classification of tumour regions in breast TMA images compared to a classification approach which incorporates no context. Classification can be improved at boundaries of TMA spots by only incorporating context within TMA spot regions.

In future work, spin-context could be compared to other state-of-the-art tumour segmentation methods. Furthermore, due to the nature of errors presented in this paper, classification around tumour boundaries also requires further investigation. It will also be useful to

investigate other image features for tumour identification and evaluate the performance of spin-context when such features are incorporated.

Acknowledgements

This work was supported by the Chief Scientist Office (grant no. CZB/4/761); and the Engineering and Physical Sciences Research Council (DTA grant).

References

S. Akbar, T. Amaral, S. J. McKenna, A. Thompson, and L. Jordan. Tumour segmentation in breast tissue microarray images using spin-context. In *Proc. Medical Image Understanding and Analysis*, pages 25–30. BMVA, 2012.

P. Chomphuwiset, D. Magee, R. Boyle, and D. Treanor. Context-based classification of cell nuclei and tissue regions in liver histopathology. In *Proc. Medical Image Understanding and Analysis*. BMVA, 2011.

N.M.T. Jawhar. Tissue microarray: A rapidly evolving diagnostic and research tool. *Annals of Saudi Medicine*, 29(2):123–127, 2009.

E. Jurrus, A.R.C. Paiva, S. Watanabe, J.R. Anderson, B.W. Jones, R.T. Whitaker, E.M. Jorgensen, R.E. Marc, and T. Tasdizen. Detection of neuron membranes in electron microscopy images using a serial neural network architecture. *Medical Image Analysis*, 14 (6):770–783, 2010.

B. Karaçali and A. Tözeren. Automated detection of regions of interest for tissue microarray experiments: an image texture analysis. *BMC Medical Imaging*, 7(1):2, 2007.

J. Kononen, L. Bubendorf, A. Kallionimeni, M. Bärlund, P. Schraml, S. Leighton, J. Torhorst, M. Mihatsch, G. Sauter, and O. Kallionimeni. Tissue microarrays for high-throughput molecular profiling of tumor specimens. *Nature Medicine*, 4(7):844–847, 1998.

S. Lazebnik, C. Schmid, and J. Ponce. A sparse texture representation using local affine regions. *IEEE Trans. on Pattern Analysis and Machine Intelligence*, 27(8):1265–1278, 2005.

H. Moch, J. Kononen, O. Kallioniemi, and G. Sauter. Tissue microarrays: what will they bring to molecular and anatomic pathology? *Advances in anatomic pathology*, 8:14–20, 2001.

A. Montillo, J. Shotton, J. Winn, J. Iglesias, D. Metaxas, and A. Criminisi. Entangled decision forests and their application for semantic segmentation of CT images. In *Information Processing in Medical Imaging*, pages 184–196. Springer, 2011.

J.H. Morra, Z. Tu, L.G. Apostolova, A.E. Green, C. Avedissian, S.K. Madsen, N. Parikshak, X. Hua, A.W. Toga, C.R. Jack Jr, M.W. Weiner, P.M. Thompson, and Alzeimer's Disease Neuroimaging Initiative. Validation of a fully automated 3D hippocampal segmentation method using subjects with alzheimer's disease mild cognitive impairment, and elderly controls. *Neuroimage*, 43(1):59–68, 2008.

N. Otsu. A threshold selection method from gray-level histograms. *Systems, Man and Cybernetics, IEEE Trans. on*, 9(1):62 –66, 1979.

C. Schmid and R. Mohr. Matching by local invariants. Technical Report RR-2644, INRIA, 1995.

Y. Tao, L. Lu, M. Dewan, A. Chen, J. Corso, J. Xuan, M. Salganicoff, and A. Krishnan. Multi-level ground glass nodule detection and segmentation in CT lung images. In *Medical Image Computing and Computer-Assisted Intervention*, pages 715–723. Springer, 2009.

Z. Tu and X. Bai. Auto-context and its application to high-level vision tasks and 3D brain image segmentation. *IEEE Trans. on Pattern Analysis and Machine Intelligence*, 32(10):1744–1757, 2010.

D. Voduc and T.O. Nielsen. Tissue microarray in clinical oncology. *Seminars in Radiation Oncology*, 18(2):89–97, 2008.

C. Wang, D. Fennel, I. Paul, K. Savage, and P. Hamilton. Robust automated tumour segmentation on histological and immunohistochemical tissue images. *PLoS ONE*, 6(2):e15818, 2011.

Y. Xu, J. Zhang, E.I. Chang, M. Lai, and Z. Tu. Context-constrained multiple instance learning for histopathology image segmentation. In *Proc. Medical Image Understanding and Analysis*, pages 623–630. BMVA, 2012.